

---

This is an electronic reprint of the original article.

This reprint may differ from the original in pagination and typographic detail.

Author(s): Jussila, H. & Nagarajan, S. & Huhtio, T. & Lipsanen, Harri & Tuomi, T. O. & Sopanen, M.

Title: Structural study of GaP layers on misoriented silicon (001) substrates by transverse scan analysis

Year: 2012

Version: Final published version

**Please cite the original version:**

Jussila, H. & Nagarajan, S. & Huhtio, T. & Lipsanen, Harri & Tuomi, T. O. & Sopanen, M. 2012. Structural study of GaP layers on misoriented silicon (001) substrates by transverse scan analysis. *Journal of Applied Physics*. Volume 111, Issue 4. P. 043518/1-6. ISSN 0021-8979 (printed). DOI: 10.1063/1.3686711.

Rights: © 2012 American Institute of Physics. This article may be downloaded for personal use only. Any other use requires prior permission of the author and the American Institute of Physics.  
<http://scitation.aip.org/content/aip/journal/jap>

---

All material supplied via Aaltodoc is protected by copyright and other intellectual property rights, and duplication or sale of all or part of any of the repository collections is not permitted, except that material may be duplicated by you for your research use or educational purposes in electronic or print form. You must obtain permission for any other use. Electronic or print copies may not be offered, whether for sale or otherwise to anyone who is not an authorised user.

## Structural study of GaP layers on misoriented silicon (001) substrates by transverse scan analysis

H. Jussila, S. Nagarajan, T. Huhtio, H. Lipsanen, T. O. Tuomi, and M. Sopanen

Citation: [Journal of Applied Physics](#) **111**, 043518 (2012); doi: 10.1063/1.3686711

View online: <http://dx.doi.org/10.1063/1.3686711>

View Table of Contents: <http://scitation.aip.org/content/aip/journal/jap/111/4?ver=pdfcov>

Published by the [AIP Publishing](#)

---

### Articles you may be interested in

[Heteroepitaxy of GaAs on \(001\)  \$\Rightarrow\$  6° Ge substrates at high growth rates by hydride vapor phase epitaxy](#)

[J. Appl. Phys.](#) **113**, 174903 (2013); 10.1063/1.4803037

[GaP heteroepitaxy on Si\(001\): Correlation of Si-surface structure, GaP growth conditions, and Si-III/V interface structure](#)

[J. Appl. Phys.](#) **111**, 083534 (2012); 10.1063/1.4706573

[In situ antiphase domain quantification applied on heteroepitaxial GaP growth on Si\(100\)](#)

[J. Vac. Sci. Technol. B](#) **28**, C5H1 (2010); 10.1116/1.3466529

[Morphological aspects of continuous and modulated epitaxial growth of \(GaIn\)P](#)

[J. Appl. Phys.](#) **88**, 3341 (2000); 10.1063/1.1288698

[Crystal tilting in GaN grown by pendeoepitaxy method on sapphire substrate](#)

[Appl. Phys. Lett.](#) **75**, 4109 (1999); 10.1063/1.125552

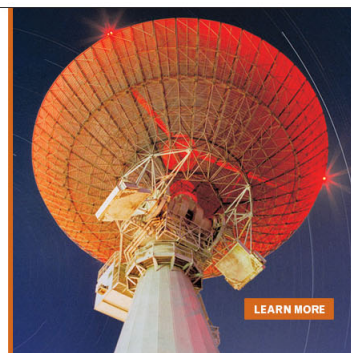
---

MIT LINCOLN  
LABORATORY  
CAREERS

Discover the satisfaction of  
innovation and service  
to the nation

- Space Control
- Air & Missile Defense
- Communications Systems & Cyber Security
- Intelligence, Surveillance and Reconnaissance Systems
- Advanced Electronics
- Tactical Systems
- Homeland Protection
- Air Traffic Control

 **LINCOLN LABORATORY**  
MASSACHUSETTS INSTITUTE OF TECHNOLOGY



LEARN MORE

# Structural study of GaP layers on misoriented silicon (001) substrates by transverse scan analysis

H. Jussila,<sup>a)</sup> S. Nagarajan, T. Huhtio, H. Lipsanen, T. O. Tuomi, and M. Sopanen

*Department of Micro and Nanosciences, Aalto University, P.O. Box 13500, FI-00076 Aalto, Finland*

(Received 24 October 2011; accepted 19 January 2012; published online 24 February 2012)

This paper examines the structural properties of gallium phosphide layers by high resolution x-ray diffraction and atomic force microscopy measurements. GaP layers are grown on misoriented and nominally exactly oriented silicon (001) substrates by metalorganic vapor phase epitaxy. Structural characterization is performed by reciprocal lattice map and transverse scan measurements of (00 $l$ )-reflections ( $l = 2, 4, 6$ ). Transverse scan line profiles of GaP layers on exactly oriented and misoriented substrates are compared thoroughly and antiphase disorder related satellite peaks are observed on exactly oriented substrates. In addition, results imply that antiphase disorder is self-annihilated on misoriented substrates. The dependence of crystallographic tilt on growth temperature indicates structural coherence. Williamson-Hall-like plot of transverse scans reveals the lateral correlation length of crystalline defects of 79 nm which gives the average size of the mosaic crystallites. In addition, the mosaicity of the GaP layer is 0.042°. © 2012 American Institute of Physics. [doi:10.1063/1.3686711]

## I. INTRODUCTION

Monolithic integration of III-V compound semiconductor thin films on low-cost and large scale silicon substrates provides means to fabricate numerous interesting devices on a single substrate. In order to successfully realize this, a suitable buffer layer has to be fabricated. The buffer layer has to be atomically smooth and possess high crystal quality with low defect density. Therefore, GaP is a promising buffer layer material due to the small lattice mismatch of 0.37% at room temperature which ensures that a thin GaP film can be grown without significant degradation of the crystal quality. In addition to this, the buffer layer has to be free of antiphase domains (APD) which are generated in III-V compound thin films due to the polarity difference with respect to the silicon substrate.

It is well-known that APD problems can be solved if the GaP layer is grown on biatomically stepped silicon substrates. Recently, it was shown that biatomic steps can be achieved on exactly oriented silicon substrates by thermal annealing of the metalorganic vapor phase epitaxy (MOVPE) grown silicon layer.<sup>1,2</sup> As a result, fabrication of a monolithically integrated high-quality semiconductor laser was demonstrated.<sup>3</sup> In addition, atomic step doubling is achieved spontaneously on silicon (001) substrates with surface miscut of over 4 deg toward the [110] direction. This approach is much more simple and requires no sensitive annealing process.<sup>4-7</sup> However, solving APD problems is not sufficient for fabrication of a high-quality layer. Other issues may also degrade the crystal quality. For instance, the lattice mismatch generates residual strain and, thus, also misfit dislocations.<sup>6</sup> In addition, the structural properties of the GaP layer may degrade due to many differences between the materials. Therefore, in order to achieve a high-quality buffer layer it is

important to understand structural defects and dislocations in the GaP layer and to minimize their formation.

In this paper, the structural properties of GaP layers on silicon are examined by high resolution x-ray diffraction (HRXRD) and atomic force microscopy (AFM) measurements. Characterization of structural properties is performed by HRXRD studies of (00 $l$ )-reflections (where  $l = 2n$ ,  $n$  integer). A complete comparison between the transverse scan line profiles of GaP layers on exactly oriented and misoriented silicon substrates is performed and antiphase disorder related satellite peaks are observed. The information concerning the strain and layer mosaicity is extracted with the reciprocal lattice map (RLM) measurements and with the Williamson-Hall-like (WHL) plots<sup>8</sup> of transverse scan line profiles, respectively. RLM studies reveal information about the strain conditions of GaP layers. WHL plots provides estimates for the lateral correlation length of crystalline defects and the crystal mosaicity.

## II. EXPERIMENT

GaP layers were grown on silicon (001) substrates by atmospheric pressure MOVPE. Silicon substrates had a miscut of 4° toward the [110] direction. Substrates with this off-cut are called misoriented substrates in this report. In addition to this, GaP films were grown on nominally exactly oriented silicon (001) substrates (a miscut less than 0.1° off the [100] direction). Tertiarybutylphosphine (TBP) and trimethylgallium (TMGa) were used as source materials. GaP was grown by a two-step growth method.<sup>1,9</sup> First, a nominally 5-nm-thick low-temperature nucleation layer (NL) was grown at 475 °C. All the temperatures mentioned in this report are thermocouple readings. Then, the reactor temperature was ramped up to grow a 75-nm-thick GaP layer under many different V/III ratios and growth temperatures to examine the effects of different growth conditions on the

<sup>a)</sup>Electronic address: henri.jussila@aalto.fi.

properties of the GaP layer. More information about the growth process can be found in Ref. 9.

GaP layers were characterized by AFM and HRXRD measurements. Transverse scan and RLM measurements were performed for (00 $l$ ) reflections ( $l = 2, 4, 6$ ). Transverse scan refers to the measurement of a high-resolution rocking curve. Thus, HRXRD measurements were performed using a triple-axis geometry. The incident beam was guided through a Ge (220) monochromator and an x-ray mirror. The zero azimuth angle was set along the substrate miscut toward the [110]-direction. The measured curves were plotted in reciprocal space units obtained by the following formulas:

$$S = \frac{2}{\lambda} \sin\left(\frac{2\theta}{2}\right), \quad (1)$$

$$S_x = S \sin(\omega - \omega_B), \quad (2)$$

where  $S$  is the diffraction vector length and  $S_x$  the diffraction vector component along the crystal plane. It should be noted that  $2\pi$  factor is removed to obtain a direct correlation between the distances in reciprocal and in direct space.<sup>4</sup> In addition,  $\omega_B$  is the  $\omega$  angle corresponding the Bragg reflection and  $\lambda$  the x-ray wavelength.

Transverse scan line profiles can possess two-component lineshapes in which the narrow component is the Bragg peak of the sample (originating from long-range structural correlations). The broad component arises from diffuse scattering and contains information about the disorder in the crystals. Two parameters are defined to estimate the origin of the disorder: (1) integral breadth (IB) of the broad component, and (2) quality factor (QF) of the line profile, defined as the ratio between the areas of the thin and broad components. Two extreme limits of disorder are strong and weak disorder. Dislocations can induce weak disorder in the crystal. On the other hand, strong disorder is typically observed in amorphous materials. However, strain in crystals can also create rotational disorder (i.e., mosaicity) which is observed at the strong disorder limit.<sup>10,11</sup>

The relation between the line shape of (00 $l$ )-reflection and index  $l$  can be used to define what is causing the disorder. Typically, weak disorder is manifested as a prominent Bragg component. In addition, the width of the broad component is constant in units of  $S_x$ .<sup>11</sup> Thus, IB stays constant as a function of increasing  $l$ . On the other hand, strong disorder created by crystal mosaicity may make the higher order reflection Bragg peaks invisible. Furthermore, the angular width of diffuse scattering is then typically constant and independent of  $S_z$  (Ref. 11) (the diffraction vector component perpendicular the crystal plane) causing IB to increase and QF to decrease as a function of  $l$ . However, the diffuse scattering arising from real crystals can very rarely be attributed to originate purely from strong or weak disorder and it is most likely an intermediate case of the both. It should also be mentioned that thermal vibration of the atoms creates diffuse scattering. However, the differences in transverse scan line profiles are not created by the effects of the temperature as all the measurements were performed at room temperature. In addition to this, if antiphase disorder is present it

affects the diffuse scattering of the APD sensitive reflections.<sup>12</sup> Thus, the QF of the APD sensitive (002) and (006) reflections is significantly lower than the QF of the APD insensitive (004) reflection when antiphase disorder exists in GaP layers.<sup>4</sup>

A WHL plot<sup>8,13</sup> was drawn to examine the origin of the diffuse scattering. The WHL plot utilizes the information carried by the broad component and differentiates the effects of laterally correlating crystalline defects and crystal mosaicity on the line shape. Two pseudo-Voigt functions were fitted to the measured curves to distinguish the broad and thin components from the line profile. The lateral correlation length of crystalline defects and crystal mosaicity was defined utilizing IB. IB and  $S_z$  obey the following fundamental equation (to an accuracy of within 5%).<sup>8</sup>

$$\left(\frac{IB}{S_z}\right)^2 = \frac{1}{\xi^2} + M^2, \quad (3)$$

where  $M$  and  $\xi$  are the mosaicity and the lateral correlation length of the crystalline defects, respectively. It should be noted that the WHL plot assumes that the correlation length is obtained by Scherrer's relation. Therefore, the lateral correlation length is similar to the average size of the mosaic crystallites.<sup>8</sup>

### III. RESULTS AND DISCUSSION

#### A. Optimization of layer morphology

Early studies of GaP growth on silicon showed that the growth mode of GaP changes from Volmer-Weber-type (VW-type) island growth to layer-by-layer type growth with increased V/III ratio.<sup>5</sup> However, the effects of increased V/III ratio are not similar when TBP is used as the group V precursor (compared to PH<sub>3</sub>). For instance, we have reported that GaP forms a layer comprised of a net of horizontal wires under typical MOVPE growth conditions.<sup>9</sup> As a result, in order to obtain high-quality GaP layer on silicon a scheme to launch two-dimensional growth immediately at the beginning of the growth is required. Otherwise, dislocations and stacking faults are generated at the locations where the VW-type islands or the GaP wires coalesce.

GaP layers were grown by two-step growth method on misoriented silicon substrates.<sup>1,9</sup> The relation between the growth conditions and layer morphology was examined by growing GaP layers at different temperatures and V/III ratios. Figure 1 presents the morphology of a 75-nm-thick GaP layer grown at different temperatures. It can be observed that the surface of GaP is extremely rough when the growth temperature is 600 °C. This is most likely due to the too low surface mobility of gallium adatoms. Due to the poor layer morphology, we have not analyzed this sample further. The GaP surface gets smoother with increasing temperature, and the smoothest surface is observed when the growth temperature is 680 °C. Then, the surface is comprised of hillocks whose height is a few nanometers. Figure 2(a) shows an AFM image of the GaP sample grown at 700 °C. It can be seen that the hillocks start to elongate toward the [110] crystal direction. The relation between the V/III ratio



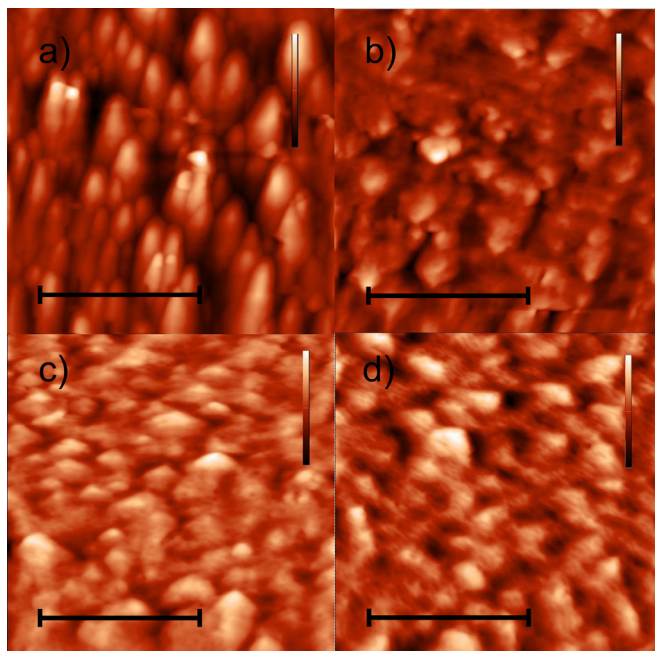


FIG. 1. (Color online) AFM images show the morphology of a 75-nm-thick GaP layer grown at (a) 600 °C, (b) 650 °C, (c), 665 °C, and (d) 680 °C on misoriented silicon (001) substrates. The color scale of the images is (a) 82 nm, (b) 20 nm, (c) 24 nm, and (d) 15 nm. The length bar of each image corresponds to a distance of 1  $\mu\text{m}$ .

and layer morphology was also examined by AFM (AFM images not shown here). The smoothest surface was observed at the highest V/III ratio of 280. The RMS roughness of the smoothest GaP layer was 1.6 nm.

## B. Antiphase disorder in GaP layers

APDs degrade the crystal quality of GaP layers. The formation of APDs should be hindered on silicon (001) substrates with surface miscut over  $4^\circ$  along the  $[110]$  direction.<sup>4,7</sup> This is due to the biatomic steps which are formed spontaneously on these surfaces. However, it should be mentioned that there always exist atomic steps with monoatomic height on misoriented substrates although the formation of biatomic steps is favored. Therefore, in order to obtain good crystal quality APDs created at these locations should be self-annihilated. The step doubling is not occurring spontaneously on exactly oriented silicon (001) surfaces.

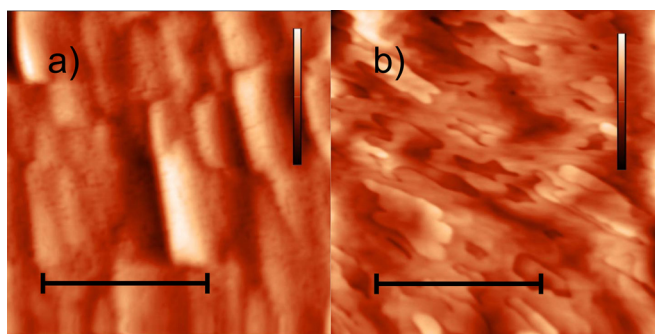


FIG. 2. (Color online) AFM images show the morphology of a 75-nm-thick GaP layer grown on (a) misoriented and (b) exactly oriented silicon (001) substrates at 700 °C. The color scale of the images is (a) 21 nm and (b) 7 nm. The length bar corresponds to a distance of 1  $\mu\text{m}$ .

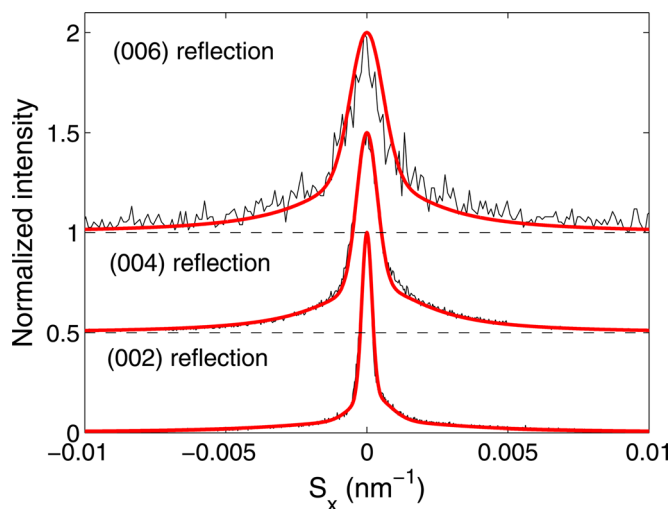


FIG. 3. (Color online) Transverse scan line profiles of (002), (004), and (006) reflections of a 75-nm-thick GaP film grown on  $4^\circ$ -off-oriented silicon (001) substrates at 700 °C. The black and red curves correspond to the measured and simulated curves, respectively. Curves from (004) and (006) reflections are moved vertically 0.5 and 1 units, respectively.

Figure 2 presents the morphology of 75-nm-thick GaP layers grown on exactly oriented and misoriented substrates with the same growth parameters. It can be seen from the image that the GaP layer grown on the exactly oriented substrate is comprised of terraces with a mean spacing of the order of 150 nm, most likely originating from antiphase disorder.

Transverse scan line profiles of GaP layers grown at 700 °C on exactly oriented and misoriented silicon substrates were compared to obtain information on APDs. Figures 3 and 4 present the measured transverse scans of (002), (004), and (006) reflections of both samples. Two-component line shape is clearly visual although the Bragg component of the GaP layer grown on the misoriented substrate has broad ended and the peak width is larger than resolution limited width. In addition to this, it can be observed that the transverse scan line profiles of the GaP layers grown on

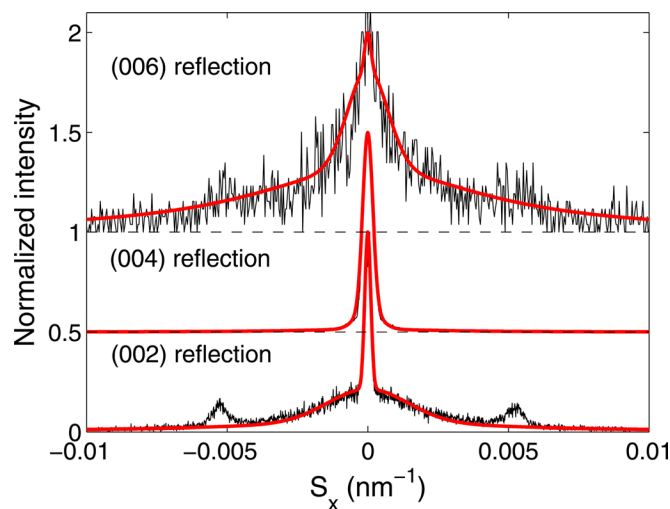


FIG. 4. (Color online) Transverse scan line profiles of (002), (004), and (006) reflections of 75-nm-thick GaP films grown on exactly oriented silicon (001) substrates at 700 °C. The black and red curves correspond to the measured and simulated curves, respectively. Curves from (004) and (006) reflections are moved vertically 0.5 and 1 units, respectively.

misoriented substrates broaden with increasing  $l$ . On the other hand, the broad component in the transverse scan line profiles of (002) and (006) reflections of the GaP layers grown on exactly oriented substrates is more prominent than the broad component of (004) reflection. Furthermore, the Bragg component of (006) reflection is almost invisible which implies strong disorder originating from sample mosaicity. In addition, satellite peaks whose origin is discussed later in this report are observed in (002) transverse scans and can also be recognized from (006) reflection.

Figure 5 shows QF and IB extracted from the transverse scan measurements. It can be observed that QF of the APD sensitive (002) and (006) reflections is significantly smaller than QF of the APD insensitive (004) reflection for the GaP layers grown on exactly oriented substrates indicating the existence of antiphase disorder. On the other hand, QF of the GaP layer grown on misoriented substrate is constant. In addition, IB increases with increasing  $l$ . This implies that the antiphase disorder of the sample is self-annihilated and that diffuse scattering cannot be defined to originate purely from strong or weak disorder.

It has been recently shown that utilizing Scherrer's relation to IB of APD sensitive reflection yields the same result for the APD size as can be obtained by TEM.<sup>4</sup> Thus, an estimate of 149 nm is obtained for the average APD size of the GaP film on the exactly oriented substrate when Scherrer's relation is applied to IB of (002) reflection. The obtained value is comparable to the terrace spacing observed from AFM images. Furthermore, the lateral correlation length of crystalline defects in an exactly oriented substrate was extracted from the WHL plot (not shown here) of APD sensitive reflections to be  $151 \pm 10$  nm which is also in the order of the terrace size. This implies that the lateral correlation length is also comparable to the mean APD size. However, it should be noted that other defects than APDs can also contribute to the correlation length.

Satellite peaks are sometimes observed in transverse scan measurements and can originate from very strong short range correlations.<sup>14</sup> For instance, previous studies of ZnO have shown satellite peaks in (002) reflections measured at two perpendicular azimuth angles. These satellite peaks were attrib-

uted to periodic arrangement of misfit or threading dislocations.<sup>8</sup> On the other hand, satellite peaks observed at (002) transverse scans of niobium layers were only seen at specific azimuth angles. In this case, satellite peaks were proposed to originate from the periodical distortion which arises from substrate miscut.<sup>15</sup> To examine the origin of the satellite peaks observed in (002) and (006) reflections a transverse scan was performed at an azimuth angle of  $90^\circ$  perpendicular to the first measurement. Satellite peaks were not observed anymore under these conditions. If these satellite peaks originate from dislocations it would mean that they should be observed at every azimuth angle or that the strong correlation between dislocations would only be along one direction.

Back-reflection x-ray diffraction topographs were measured with synchrotron radiation to search for dislocations. No dislocations were observed which gives further evidence that the origin of the satellite peaks is most likely periodic distortion arising from the terraces on the surface of the substrate. The origin of APDs is also the atomic terraces of the silicon substrate. Therefore, the observed satellite peaks may be related to antiphase disorder. Calculated mean period from the satellite peaks<sup>14</sup> for the distortion is 190 nm which is close to the APD size obtained by the Scherrer's relation or from the AFM images.

### C. Strain and mosaicity in GaP layers

Strain conditions of the GaP layers were examined by reciprocal lattice map measurements. Figure 6 presents the RLMs performed at  $\psi = 0^\circ$  and  $\psi = 90^\circ$  azimuth angles for a GaP sample grown at  $700^\circ\text{C}$  on a misoriented substrate. Two peaks exist in both RLMs with the larger peak at a  $2\theta$  angle of  $69.13^\circ$  originating from the silicon substrate and the other at  $68.60^\circ$  from the GaP layer. The  $2\theta$  angle corresponding to the (004)-reflection of bulk GaP is  $68.84^\circ$  which differs significantly from the measured value. This means that the fabricated GaP layer is compressively strained in the surface plane. The obtained value for the  $2\theta$  angle of GaP (004) reflection agrees well with the previous reports of GaP layers with comparable thickness grown on misoriented silicon substrates.<sup>6</sup>

Previously, it has been reported that when GaP is grown on misoriented silicon substrates tilt appears between the

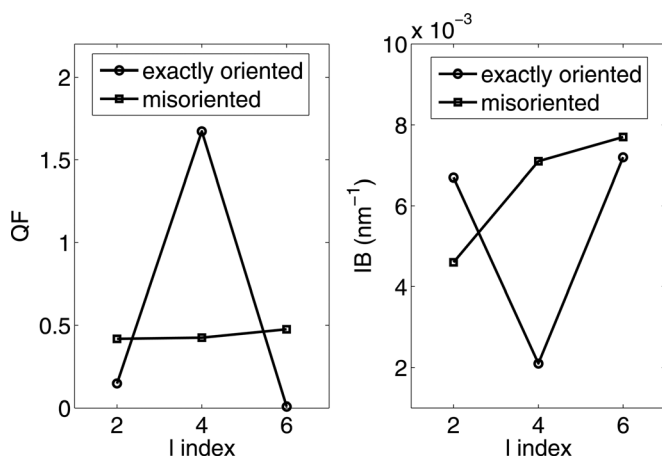


FIG. 5. Quality factor (left) and integral breadth (right) extracted from (002), (004) and (006) reflections.

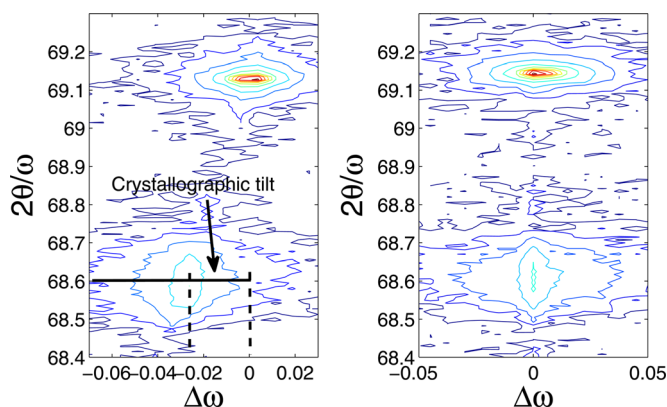


FIG. 6. (Color online) Reciprocal lattice maps of a 75-nm-thick GaP film grown at  $700^\circ\text{C}$  on a misoriented substrate measured at an azimuth angle of (a)  $\psi = 0^\circ$  and (b)  $\psi = 90^\circ$ .

GaP and silicon crystal planes along the substrate miscut direction.<sup>6</sup> The crystallographic tilt is originating from an attempt of the film to relieve strain. Strain arises from the lattice mismatch and the substrate miscut provides a means for the GaP layer to relieve the strain by tilting the GaP crystal planes away from the silicon crystal planes without formation of misfit dislocations. The relation between the crystallographic tilt and the growth temperature was measured by XRD to examine the relaxation of the GaP layers.

Figure 7 shows the measured crystallographic tilt as a function of growth temperature. It can be seen that the crystallographic tilt is increasing with increasing growth temperature. This can be explained by the increased strain at the growth temperature due to the significant difference of thermal expansion coefficients of GaP ( $4.65 \times 10^{-6}/^{\circ}\text{C}$ ) and silicon ( $2.6 \times 10^{-6}/^{\circ}\text{C}$ ). The crystallographic tilt of a coherent crystal has been shown to correlate to the strain conditions of GaP layers and increases with increased strain.<sup>6</sup> The theoretical crystallographic tilt of a coherent crystal was calculated with the Nagai's model<sup>16</sup> at growth temperature and is plotted in Fig. 7 as a comparison. It can be seen that the theoretical crystallographic tilt increases with increasing growth temperature with quite a similar slope as the measured data indicating structural coherence. However, the calculated tilt is larger which may imply that the GaP film also relieves strain by formation of misfit dislocations. It should be noted that the critical thickness of GaP on silicon for formation of misfit dislocations has previously been reported to be in the order of 95 nm<sup>6,17</sup> which indicates that no misfit dislocations should exist in the GaP film. However, further structural study is required to reveal the existence of misfit dislocations in the GaP film. On the other hand, the crystallographic tilt may also change during the cooling down process due to reduced thermal strain.

Transverse scan line profiles of a GaP layer grown at 680 °C were measured to investigate the disorder in the GaP layer induced by defects and film mosaicity. It should be noted that the surface morphology of this sample was the

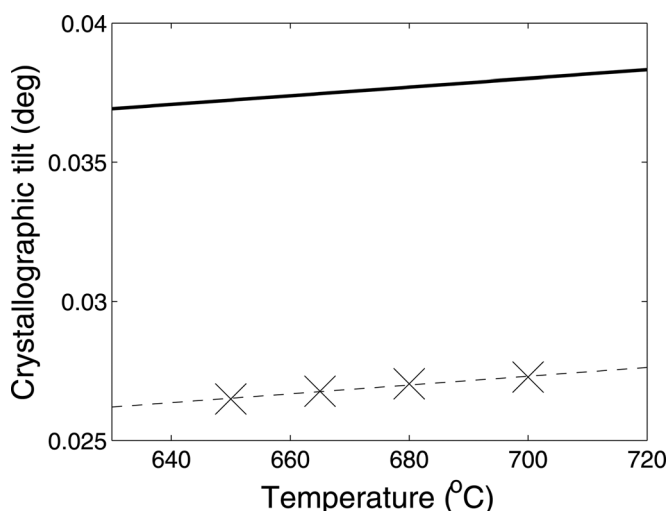


FIG. 7. Measured crystallographic tilt (×) as a function of growth temperature. The solid line plots the calculated theoretical tilt calculated from the Nagai's model. The dashed line illustrates the trend line obtained by fitting a first degree polynomial to the data.

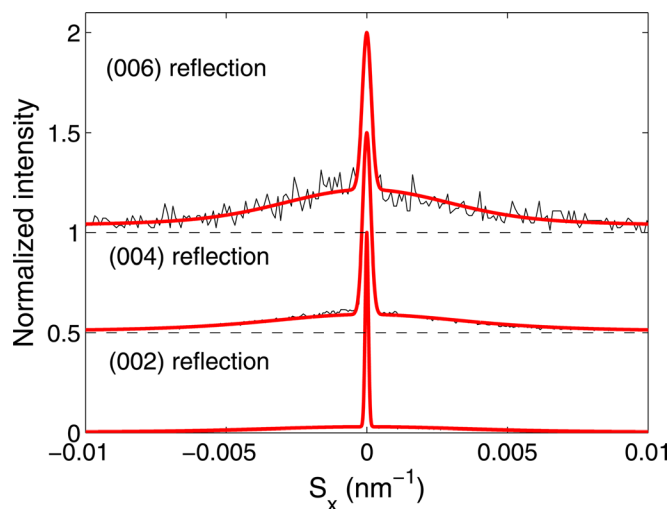


FIG. 8. (Color online) Transverse scan line profiles of (002), (004), and (006) reflections of a 75-nm-thick GaP film grown on misoriented silicon (001) substrates at 680 °C. The black and red curve correspond to the measured and simulated curves, respectively. Curves from (004) and (006) reflections are moved vertically by 0.5 and 1 units, respectively.

smoothest and also the crystal quality of this sample was the highest based on the HRXRD measurements. Transverse scan line profiles of the sample grown at 680 °C are shown in Fig. 8. The two-component line shape can easily be recognized and it should be noted that now the width of the Bragg reflection ( $0.003^{\circ}$ ) is close to the resolution limited width. In addition, it should be mentioned that IB of (002) and (004) reflections is constant indicating weak disorder in the sample. This implies that diffuse scattering is dominated by crystalline defects.

The lateral correlation length of crystalline defects and layer mosaicity were extracted from the WHL plot to examine the mosaicity of the GaP layer. Figure 9 presents the WHL plot. The obtained correlation length of  $79 \pm 7$  nm originates from the displacements in the crystal lattice induced by the crystalline defects and provides an estimate

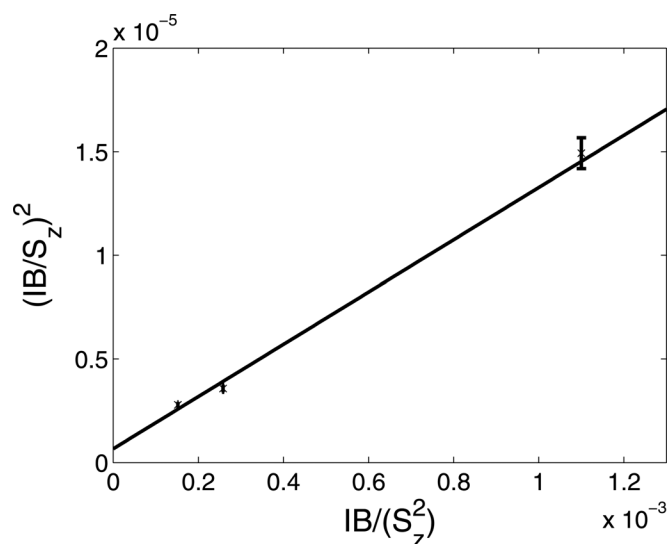


FIG. 9. Williamson-Hall-like plot of the GaP layer grown at 680 °C on misoriented silicon (001) substrate.



for the average mosaic size of the layer. However, the weak disorder implies that long range correlations are maintained in the crystal over the mosaic grain boundaries. Therefore, it is of interest to understand the physical origin of the observed mosaic crystallites in the GaP layer. For instance, misfit or threading dislocations tend to arrange periodically in a crystal in order to reduce their elastic energy and may create mosaicity. However, as it was concluded earlier it is probable that the thickness of the GaP film has not exceeded the critical thickness and that no misfit dislocations should exist in GaP layer. Thus, mosaicity is most likely created by other type of crystalline defects than misfit dislocations. The obtained value for film mosaicity of  $0.042 \pm 0.006^\circ$  is smaller compared to the other reported values of  $0.215^\circ$  (Ref. 13) and  $0.103^\circ$  (Ref. 7) for GaP on misoriented silicon substrates. The different growth conditions, growth method or film thicknesses may explain the difference.

#### IV. CONCLUSIONS

The structural properties of GaP layers on silicon were examined by HRXRD and AFM measurements. The AFM measurements showed that the surface of the GaP layer on a misoriented substrate consists of hillocks with different size depending on the growth parameters. In addition, it was observed that the roughness of the GaP layers decreased with increasing growth temperature and V/III ratio. The RMS roughness of the smoothest GaP film was 1.6 nm. On the other hand, the AFM study of GaP films on exactly oriented substrates showed that the surface of the layers were comprised of smooth terraces. Transverse scan measurements together with the WHL plots revealed information concerning the APD structure. The obtained estimates from the transverse scan measurements for the average APD size of GaP layers on exactly oriented silicon substrates were in good agreement with the mean spacing of the terraces found in the AFM study. Satellite peaks were also observed in (002) and (006) transverse scans and are proposed to originate from the periodic distortion caused by antiphase boundaries. On the other hand, results implied that antiphase disorder was self-annihilated on misoriented silicon substrates. The dependence of the crystallographic tilt with the growth temperature

indicated structural coherence. The lateral correlation length of crystal defects provided an estimate of 79 nm for the average crystallite size of the GaP layer. In addition, the mosaicity of the GaP layer was  $0.042^\circ$ .

#### ACKNOWLEDGMENTS

The authors thank Dr. Carsten Paulmann for his assistance at HASYLAB beamline F1 Topography. The authors also acknowledge financial support by the European Community - Research Infrastructure Action under the FP6 "Structuring the European Research Area" Programme (through the Integrated Infrastructure Initiative "Integrating Activity on Synchrotron and Free Electron Laser Science") under HASYLAB project DESY-D-II-20100066 EC.

- <sup>1</sup>I. Németh, B. Kunert, W. Stolz, and K. Volz, *J. Cryst. Growth* **310**, 1595 (2008).
- <sup>2</sup>B. Kunert, I. Németh, S. Reinhard, K. Volz, and W. Stolz, *Thin Solid Films* **517**, 140 (2008).
- <sup>3</sup>S. Liebich, M. Zimprich, P. Ludewig, A. Beyer, K. Volz, W. Stolz, B. Kunert, N. Hossain, S. R. Jin, and S. J. Sweeney, *Semiconductor Laser Conference (ISLC), 2010 22nd IEEE International*, 26–30 Sept. 2010 (Kyoto, 2010), pp. 143–144.
- <sup>4</sup>A. Létoublon, W. Guo, C. Cornet, A. Bouille, M. Véron, A. Bondi, O. Durand, T. Rohel, O. Dehaese, N. Chevalier, N. Bertru, and A. L. Corre, *J. Cryst. Growth* **323**, 409 (2011).
- <sup>5</sup>T. Soga, T. Jimbo, and M. Umeno, *J. Cryst. Growth* **163**, 165 (1996).
- <sup>6</sup>Y. Takagi, Y. Furukawa, A. Wakahara, and H. Kan, *J. Appl. Phys.* **107**, 063506 (2010).
- <sup>7</sup>V. Dixit, T. Ganguli, T. Sharma, S. Singh, R. Kumar, S. Porwal, P. Tiwari, A. Ingale, and S. Oak, *J. Cryst. Growth* **310**, 3428 (2008).
- <sup>8</sup>O. Durand, A. Létoublon, D. Rogers, and F. H. Teherani, *Thin Solid Films* **519**, 6369 (2011).
- <sup>9</sup>H. Jussila, S. Nagarajan, P. Mattila, J. Riikonen, T. Huhtio, M. Sopanen, and H. Lipsanen, *Phys. Status Solidi C* (to be published).
- <sup>10</sup>P. F. Miceli and C. J. Palmstrom, *Phys. Rev. B* **51**, 5506 (1995).
- <sup>11</sup>P. Miceli, J. Weatherwax, T. Krentsel, and C. Palmstrøm, *Physica B* **221**, 230 (1996).
- <sup>12</sup>B. E. Warren, *X-Ray Diffraction* (Addison-Wesley, Reading, MA, 1969).
- <sup>13</sup>O. Durand, A. Létoublon, D. J. Rogers, F. H. Teherani, C. Cornet, and A. L. Corre, *SPIE* **7940**, 79400L (2011).
- <sup>14</sup>V. M. Kaganer, O. Brandt, H. Riechert, and K. K. Sabelfeld, *Phys. Rev. B* **80**, 033306 (2009).
- <sup>15</sup>A. Gibaud, R. A. Cowley, D. F. McMorrow, R. C. C. Ward, and M. R. Wells, *Phys. Rev. B* **48**, 14463 (1993).
- <sup>16</sup>H. Nagai, *J. Appl. Phys.* **45**, 3789 (1974).
- <sup>17</sup>T. Soga, T. Jimbo, and M. Umeno, *Jpn. J. Appl. Phys.* **32**, L767 (1993).